

Radio Map-Assisted CSI Tracking with Uncertain Locations in Massive MIMO Networks

Yuanshuai Zheng and Juntao Chen

School of Science and Engineering, Shenzhen Future Network of Intelligence Institute (FNii-Shenzhen), and
Guangdong Provincial Key Laboratory of Future Networks of Intelligence
The Chinese University of Hong Kong, Shenzhen, Guangdong 518172, P.R. China

Abstract—Massive multiple-input multiple-output (MIMO) systems offer significant potential to enhance wireless communication performance, yet efficient and accurate channel state information (CSI) tracking remains a key challenge, particularly in dynamic urban settings. To address this, we propose a radio map-assisted framework for CSI tracking and trajectory discovery, relying on sparse channel observations. The radio map is redefined as a mapping from spatial positions to deterministic channel covariance matrices, which captures the complex and time-varying characteristics of urban wireless environments. Leveraging these covariance maps, we develop a CSI tracking method that enables accurate estimation using only single-dimensional observations collected during user movement. Furthermore, we present an efficient algorithm that constructs and continuously refines the radio map through sequential sparse observations, even when location labels are uncertain. Numerical results based on real city maps and ray-tracing MIMO channel datasets show that the proposed framework significantly outperforms baseline methods in both accuracy and adaptability.

Index Terms—Massive MIMO, CSI tracking, radio map, trajectory discovery, channel covariance map

I. INTRODUCTION

Massive multiple-input multiple-output (MIMO) technology has emerged as a cornerstone for enhancing the capacity and reliability of next-generation wireless communication systems, including 5G and beyond networks. By equipping base stations with large antenna arrays, massive MIMO enables the simultaneous transmission of multiple data streams to multiple users, dramatically improving spectral efficiency [1]–[3]. A key enabler of these performance gains is accurate channel state information (CSI), which allows for optimal beamforming, resource allocation, and interference management [2], [4]. However, acquiring accurate CSI in real-time is a challenging task, particularly in dynamic environments where users are highly mobile.

Conventional CSI tracking techniques often rely on high-dimension and frequent observations, which may not be

feasible in real-world scenarios where the number of radio-frequency (RF) chains is much smaller than that of antennas, the user is moving in a relatively high speed, and the number of pilots is limited due to communication efficiency. Some existing works on CSI tracking focus on exploiting either the time-domain or the spatial-domain properties of channels to enhance estimation accuracy. Approaches such as Kalman filter [5]–[7], Turbo compressive sensing (CS) [8], autoregressive (AR) models [9] or long-short term memory (LSTM) networks [10]–[12] have been widely adopted to predict CSI based on temporal correlations between successive observations. While these methods have shown promise in time-series prediction, they typically assume high-dimension or full-dimension channel observations at every location, which can be impractical in large-scale MIMO systems. Some other works adopted deep learning methods, such as attention networks [6], [13], reinforcement learning [14], convolutional neural networks [15], or generative models [16], to perform CSI estimation while they require a lot of pilots for training, and their performance in high speed scenario is unknown. In Massive MIMO systems, acquiring full-dimensional CSI during user movement requires an extensive number of pilot signals, significantly increasing overhead and reducing the system's overall efficiency.

Additionally, most of the existing techniques [5], [7], [14], [17]–[23] are based on empirical and parametric channel models under line-of-sight (LOS) conditions while they do not take the actual blockage environment into account. Although some works [3], [24]–[26] describe the non-line-of-sight (NLOS) channels using explicit array response vector and estimate the LOS path component and NLOS path component, separately, the gap between the proposed NLOS channel models and the actual channel is unknown.

Another common assumption in the literature [27]–[29] is the availability of precise location labels to assist in CSI tracking and estimation. Many studies integrate location information to improve channel prediction, leveraging the spatial relationship between user position and CSI. However, these methods rely on accurate location data, which may not always be available, especially in dynamic and complex environments. Inaccurate or missing location labels can severely degrade the performance of these techniques. Recent works in channel charting [30], [31] offer a promising alternative by enabling CSI tracking without requiring explicit knowledge of user locations. Channel charting maps high-dimensional CSI data

Juntao Chen is the corresponding author. The work was supported in part by the Basic Research Project No. HZQB-KCZY2021067 of Hetao Shenzhen-HK S&T Cooperation Zone, by the National Science Foundation of China under Grant No. 62171398 and No. 62293482, by the Shenzhen Science and Technology Program under Grant No. JCYJ20220530143804010, No. KQTD20200909114730003, and No. KJZD20230923115104009, by Guangdong Research Projects No. 2019QN01X895, No. 2017ZT07X152, and No. 2019CX01X104, by the Shenzhen Outstanding Talents Training Fund 202002, by the Guangdong Provincial Key Laboratory of Future Networks of Intelligence (Grant No. 2022B121010001), by the National Key R&D Program of China with grant No. 2018YFB1800800, and by the Key Area R&D Program of Guangdong Province with grant No. 2018B030338001.

to a lower-dimensional latent space, allowing for relative user movement to be inferred. However, most of these works still require complete channel observations during movement, making them impractical when the channel dimension is large. Although some works [31], [32] propose to transform the channel charting data to real-world locations, accurate reference locations and topological maps are still required.

While significant progress has been made in CSI tracking and estimation, there remains a gap in methods that can efficiently handle extremely sparse observations and uncertain location labels, particularly in the high-dimensional regime of Massive MIMO networks. Radio map offers a promising solution by leveraging spatial channel distributions to aid in CSI estimation, even under sparse observation conditions [33], [34]. Traditional radio maps are typically defined as mappings from the location vector to a value of reference signal received power (RSRP), signal-to-noise ratio (SNR) or angle of arrival (AoA) [34]. However, such a direct mapping fails to fully exploit the capabilities of MIMO systems, such as adaptive beamforming and robust communication under time-varying conditions. Therefore, in massive MIMO networks, the radio map should be able to capture the channel features from a higher dimension. Additionally, the construction of radio map requires accurate sampling location information [34], [35] while accurate locations may be unavailable due to NLOS conditions or hardware limitations.

This paper addresses the problem of CSI tracking and trajectory discovery in urban environments where multiple base station (BS)s equipped with MIMO antennas serve moving users. The primary objective is to construct radio maps for the BSs using sequential but sparse observations of channels and leverage these maps for radio map-assisted trajectory discovery and CSI estimation. The main contributions of this work are summarized as follows:

- **A New Radio Map Structure for MIMO Systems:** In this work, we define a radio map as a mapping from spatial positions to deterministic channel covariance matrices, reflecting the dynamic nature of wireless channels in urban environments.
- **Channel Covariance Map-Assisted CSI Tracking:** By exploiting the spatial distribution of the channel properties encapsulated in the channel covariance map, we show that it is sufficient to perform CSI tracking using a low-dimensional observation, *i.e.*, 1-dimension. In this setup, users move along urban roads, providing only one observation at each location. The proposed approach combines random sampling strategy and subspace exploration of channel covariance, leading to accurate tracking with sparse data.
- **Coarse Location-Based Radio Map Construction:** We propose an efficient algorithm for constructing channel covariance maps using only coarse user location information. The initial radio map is generated based on historical sequential observations, even in the presence of significant location uncertainty. As users move, the radio map is dynamically refined through the iterative execution of trajectory discovery, CSI estimation, and map reconstruction, using sparse future observations. This

adaptive framework ensures that the radio map remains effective in complex, real-world urban environments. Numerical results demonstrate the superior performance of the proposed algorithm compared to baseline methods.

II. SYSTEM MODEL

This section firstly presents the MIMO system and the channel statistical model. Then, the observation model is established. Finally, a radio map model named channel covariance map is introduced to assist in MIMO channel estimation and user localization.

A. Network Topology and Channel Model

Consider a MIMO network with Q BSs and a mobile user as shown in Fig. 1, where each BS equip with N_T antennas and the mobile user has a single antenna. The area of interest is divided into N grids, and the locations in the i th grid are collected in a set \mathcal{G}_i for $i \in \mathcal{N} \triangleq \{1, 2, \dots, N\}$. Denote the center location of the i th grid \mathcal{G}_i as \mathbf{x}_i , and all the centers of grids are collected in a set $\mathcal{X} = \{\mathbf{x}_1, \mathbf{x}_2, \dots, \mathbf{x}_N\}$.

A narrow-band multi-path MIMO channel from the BS $q \in \mathcal{Q} \triangleq \{1, 2, \dots, Q\}$ to the moving user located at \mathbf{p}_t at time t can be modeled as

$$\tilde{\mathbf{h}}_t^{(q)} = \tilde{\mathbf{h}}^{(q)}(\mathbf{p}_t) = \beta_0(\mathbf{h}_s^{(q)}(\mathbf{p}_t) + \mathbf{h}_e^{(q)}(\mathbf{p}_t))$$

where $\mathbf{h}_s^{(q)}(\mathbf{p}_t)$ is the normalized deterministic channel due to static scattering from the location \mathbf{p}_t to the BS, and $\mathbf{h}_e^{(q)}(\mathbf{p}_t)$ is the normalized random component due to moving scatters in a time-varying environment. Given the location \mathbf{p}_t lying in the i th grid, the deterministic channel $\mathbf{h}_s^{(q)}(\mathbf{p}_t)$ is assumed to satisfy $\mathbf{h}_s^{(q)}(\mathbf{p}_t) \sim \mathcal{CN}(0, \mathbf{C}_i^{(q)})$ where $\mathbf{C}_i^{(q)}$ is the channel covariance in the i th grid, and

$$\mathbf{C}_i^{(q)} = \mathbb{E}_{\mathbf{p} \in \mathcal{G}_i} \{\mathbf{h}_s^{(q)}(\mathbf{p})(\mathbf{h}_s^{(q)}(\mathbf{p}))^H\} \quad (1)$$

Additionally, it is assumed that the random component $\mathbf{h}_e^{(q)}(\mathbf{p}_t)$ of the channel at \mathbf{p}_t follows a zero-mean complex Gaussian distribution, *i.e.*, $\mathbf{h}_e^{(q)}(\mathbf{p}_t) \sim \mathcal{CN}(0, \sigma_h^2 \mathbf{I}_{N_t})$ where σ_h^2 is the variance of $\mathbf{h}_e^{(q)}(\mathbf{p}_t)$.

Removing the path loss component β_0 from $\tilde{\mathbf{h}}_t^{(q)}$, the normalized channel is denoted as

$$\mathbf{h}_t^{(q)} = \mathbf{h}^{(q)}(\mathbf{p}_t) = \beta_0^{-1} \tilde{\mathbf{h}}_t^{(q)} = \mathbf{h}_s^{(q)}(\mathbf{p}_t) + \mathbf{h}_e^{(q)}(\mathbf{p}_t). \quad (2)$$

This paper aims to estimate the normalized channel $\mathbf{h}_t^{(q)}$ as the path loss component β_0 can be estimated by many existing approaches [36].

Therefore, the channel $\mathbf{h}_t^{(q)}$ hereby with $\mathbf{p}_t \in \mathcal{G}_i$ follows a complex Gaussian distribution as

$$\mathbf{h}_t^{(q)} \sim \mathcal{CN}(0, \mathbf{C}_i^{(q)} + \sigma_h^2 \mathbf{I}_{N_t \times N_t}). \quad (3)$$

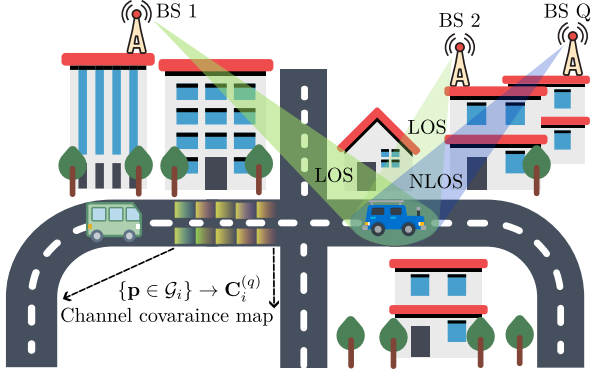


Figure 1. A MIMO system with Q BSs equipped with MIMO antennas. The users move along the roads, and sparse measurements are used for constructing a channel covariance map which is a mapping from locations $\mathbf{p} \in \mathbb{R}^3$ in the i th grid to a channel covariance matrix $\mathbf{C}_i^{(q)} \in \mathbb{R}^{N_t \times N_t}$.

B. Observation Model

Define the observation measured for the channel between the q th BS and the user location $\mathbf{p}_t \in \mathcal{G}_i$ as

$$\mathbf{y}_t^{(q)} = \mathbf{y}^{(q)}(\mathbf{p}_t) = \mathbf{A}\mathbf{h}_t^{(q)} + \mathbf{n}_t^{(q)} \quad (4)$$

where $\mathbf{A} \in \mathbb{R}^{M \times N_t}$ representing a semi-unitary sparse combining matrix satisfying $\mathbf{A}\mathbf{A}^H = \mathbf{I}_{M \times M}$, in which, $M \leq N_t$, and \mathbf{n}_t is the measurement noise. It is assumed that \mathbf{n}_t follows a zero-mean complex Gaussian distribution, i.e., $\mathbf{n}_t \sim \mathcal{CN}(\mathbf{0}, \sigma_n^2 \mathbf{I}_M)$ where σ_n is the variance of the measurement noise.

Given $\mathbf{h}_t^{(q)} \sim \mathcal{CN}(\mathbf{0}, \mathbf{C}_i^{(q)} + \sigma_h^2 \mathbf{I}_{N_t \times N_t})$ in (3), the observation $\mathbf{y}_t^{(q)}$ satisfies that

$$\mathbf{y}_t^{(q)} \sim \mathcal{CN}(\mathbf{0}, \mathbf{A}\mathbf{C}_i^{(q)}\mathbf{A}^H + (\sigma_h^2 + \sigma_n^2)\mathbf{I}_{M \times M})$$

where $\mathbf{I}_{M \times M} \in \mathbb{R}^{M \times M}$ is a unit diagonal matrix because $\mathbf{A}\mathbf{A}^H = \mathbf{I}_{M \times M}$.

For presentation convenience, let $\sigma^2 = \sigma_h^2 + \sigma_n^2$, and $\mathbf{D}_i^{(q)} = \mathbf{A}\mathbf{C}_i^{(q)}\mathbf{A}^H + \sigma^2 \mathbf{I}_{M \times M}$, and thus, $\mathbf{y}_t^{(q)} \sim \mathcal{CN}(\mathbf{0}, \mathbf{D}_i^{(q)})$ for $\mathbf{p}_t \in \mathcal{G}_i$.

Therefore, the probability density function (PDF) of the observation $\mathbf{y}_t^{(q)}$ given the user location $\mathbf{p}_t \in \mathcal{G}_i$ or the corresponding deterministic channel covariance $\mathbf{C}_i^{(q)}$ is given by

$$p(\mathbf{y}_t^{(q)}|\mathbf{p}_t) = p(\mathbf{y}_t^{(q)}|\mathbf{C}_i^{(q)}) = \frac{\exp\left\{-\left(\mathbf{y}_t^{(q)}\right)^H \left(\mathbf{D}_i^{(q)}\right)^{-1} \mathbf{y}_t^{(q)} / 2\right\}}{(2\pi)^{M/2} |\mathbf{D}_i^{(q)}|^{1/2}} \quad (5)$$

C. Radio Map Model

In a MIMO system with Q BSs, each BS construct and maintains a radio map. Different from most existing radio maps which map the location information to RSRP values or SNR values, this paper construct radio maps bridging the location information with MIMO channel distributions.

Specifically, a radio map, also called channel covariance map, for the BS $q \in \mathcal{Q}$ is proposed as

$$\mathcal{M}^{(q)} = \{(\mathbf{x}_i, \mathbf{C}_i^{(q)}), i \in \mathcal{N}\}. \quad (6)$$

Each entry $(\mathbf{x}_i, \mathbf{C}_i^{(q)})$ in the radio map $\mathcal{M}^{(q)}$ represents a specific grid center \mathbf{x}_i and its corresponding deterministic channel covariance matrix $\mathbf{C}_i^{(q)}$. The use of deterministic channel covariance $\mathbf{C}_i^{(q)}$ ensures that the radio map captures the average behavior of the channel in the i th grid centered at \mathbf{x}_i .

The proposed radio map in (6) aids in channel estimation without knowing user locations, requiring limited channel observation data. This efficiency is due to the fact that $\mathbf{C}_i^{(q)}$ already includes channel statistical knowledge. Next, this paper integrates sparse and sequential observations with the statistical data encoded in the radio map to do user trajectory discovery and channel estimation.

III. RADIO MAP-ASSISTED TRAJECTORY DISCOVERY AND CHANNEL ESTIMATION

A radio map-assisted trajectory discovery and channel estimation problem is established in this section. The trajectory discovery problem is a Hidden Markov Model (HMM) problem which can be solved by a recursive algorithm based on sparse and sequential CSI measurements. After the user trajectory is discovered, the real-time sampled CSI measurement are utilized to estimate the channel.

A. Problem for Joint Trajectory Discovery and Channel Estimation

Denote $\mathcal{Y}_t^{(q)} = \{\mathbf{y}_1^{(q)}, \mathbf{y}_2^{(q)}, \dots, \mathbf{y}_t^{(q)}\}$ as a sequence of CSI measurements collected along the user trajectory \mathcal{P}_t where \mathcal{P}_t is a location sequence, i.e., $\mathcal{P}_t = \{\mathbf{p}_1, \mathbf{p}_2, \dots, \mathbf{p}_t\}$ in which \mathbf{p}_t is the actual user location at time t .

According to the Bayes' theorem of probability, one can obtain

$$\begin{aligned} p(\mathcal{Y}_t^{(q)}, \mathcal{P}_t) &= p(\mathbf{y}_t^{(q)}|\mathcal{Y}_{t-1}^{(q)}, \mathcal{P}_t)p(\mathcal{Y}_{t-1}^{(q)}, \mathcal{P}_t) \\ &= p(\mathbf{y}_t^{(q)}|\mathbf{p}_t)p(\mathcal{Y}_{t-1}^{(q)}, \mathcal{P}_t) \end{aligned} \quad (7)$$

$$\begin{aligned} &= p(\mathbf{y}_t^{(q)}|\mathbf{p}_t)\mathbb{P}(\mathbf{p}_t|\mathcal{Y}_{t-1}^{(q)}, \mathcal{P}_{t-1})p(\mathcal{Y}_{t-1}^{(q)}, \mathcal{P}_{t-1}) \\ &= p(\mathbf{y}_t^{(q)}|\mathbf{p}_t)\mathbb{P}(\mathbf{p}_t|\mathcal{P}_{t-1})p(\mathcal{Y}_{t-1}^{(q)}, \mathcal{P}_{t-1}) \end{aligned} \quad (8)$$

$$\approx p(\mathbf{y}_t^{(q)}|\mathbf{p}_t)\mathbb{P}(\mathbf{p}_t|\mathbf{p}_{t-1})p(\mathcal{Y}_{t-1}^{(q)}, \mathcal{P}_{t-1}) \quad (9)$$

where equation (7) is due to the fact that $\mathbf{y}_t^{(q)}$ only depends on the measurement location \mathbf{p}_t and is independent of $\mathcal{Y}_{t-1}^{(q)}$ and \mathcal{P}_{t-1} , equation (8) is due to the fact that \mathbf{p}_t is independent of $\mathcal{Y}_{t-1}^{(q)}$, and (9) uses the approximation $\mathbb{P}(\mathbf{p}_t|\mathcal{P}_{t-1}) \approx \mathbb{P}(\mathbf{p}_t|\mathbf{p}_{t-1})$ to reduce the model complexity for the trajectory estimation problem to be formulated shortly.

Suppose that we take measurements $\mathcal{Y}_T^{(q)} = \{\mathbf{y}_1^{(q)}, \mathbf{y}_2^{(q)}, \dots, \mathbf{y}_T^{(q)}\}$ along the trajectory $\mathcal{P}_T = \{\mathbf{p}_1, \mathbf{p}_2, \dots, \mathbf{p}_T\}$. The joint probability density $p(\mathcal{Y}_T^{(q)}, \mathcal{P}_T)$ can be computed by recursively applying (9), and we obtain

$$p(\mathcal{Y}_T^{(q)}, \mathcal{P}_T) = \prod_{t=1}^T p(\mathbf{y}_t^{(q)}|\mathbf{p}_t) \times \prod_{t=2}^T \mathbb{P}(\mathbf{p}_t|\mathbf{p}_{t-1})\mathbb{P}(\mathbf{p}_1). \quad (10)$$

Given the radio map $\mathcal{M}^{(q)}$, the trajectory \mathcal{P}_T and the channels in $\mathcal{H}_Q = \{\mathbf{h}_T^{(1)}, \mathbf{h}_T^{(2)}, \dots, \mathbf{h}_T^{(Q)}\}$ for all the BSs can

be estimated by maximizing the log-likelihood of $p(\mathcal{Y}_T, \mathcal{P}_T)$ in (10), yielding

$$\begin{aligned} & \underset{\mathcal{P}_T, \mathcal{H}_Q}{\text{maximize}} \quad \sum_{t=1}^T \sum_{q \in \mathcal{Q}} \log p(\mathbf{y}_t^{(q)} | \mathbf{p}_t) + \sum_{t=2}^T \log \mathbb{P}(\mathbf{p}_t | \mathbf{p}_{t-1}) \quad (11) \\ & \quad + \log \mathbb{P}(\mathbf{p}_1) \\ & \text{subject to } \mathbf{p}_t \in \mathcal{X} \end{aligned}$$

$$\|\mathbf{p}_t - \mathbf{p}_{t-1}\|_2 \leq D_m, \quad \forall t \in \{2, 3, \dots, T\} \quad (12)$$

where D_m is a predetermined constant to evaluate whether \mathbf{x}_k is reachable from \mathbf{x}_i in one time slot, $\mathbb{P}(\mathbf{p}_t | \mathbf{p}_{t-1})$ is obtained from the historical user mobile properties, and the constraint $\mathbf{p}_t \in \mathcal{X}$ makes the projection from the actual use location to discrete and reference locations in \mathcal{X} . The prior probability $\mathbb{P}(\mathbf{x}_1)$ can be initialized as a constant \mathbb{P}_0 , if unknown.

B. Trajectory Discovery Using Sequential CSI Measurements

Given the radio map $\mathcal{M}^{(q)}$, the trajectory discovery problem in (11) is a standard HMM problem formulated as

$$\begin{aligned} & \underset{\mathcal{P}_T}{\text{maximize}} \quad \sum_{t=1}^T \sum_{q \in \mathcal{Q}} \log p(\mathbf{y}_t^{(q)} | \mathbf{p}_t) + \sum_{t=2}^T \log \mathbb{P}(\mathbf{p}_t | \mathbf{p}_{t-1}) \quad (13) \\ & \quad + \log \mathbb{P}(\mathbf{p}_1) \\ & \text{subject to } \mathbf{p}_t \in \mathcal{X}. \end{aligned}$$

$$\|\mathbf{p}_t - \mathbf{p}_{t-1}\|_2 \leq D_m, \quad \forall t \in \{2, 3, \dots, T\} \quad (14)$$

To make the objective function in problem (13) tractable, we establish a discrete mobility model to quantify the location state transition probability $\mathbb{P}(\mathbf{p}_t | \mathbf{p}_{t-1})$ with the constraint $\mathbf{p}_t \in \mathcal{X}$ and $\mathbf{p}_{t-1} \in \mathcal{X}$.

Consider the transition probability from the user location \mathbf{p}_{t-1} to \mathbf{p}_t . Since the actual user locations $\mathcal{P}_{t-1} = \{\mathbf{p}_1, \mathbf{p}_2, \dots, \mathbf{p}_{t-1}\}$ in the past $t-1$ time slots are unknown, the estimated user locations $\tilde{\mathcal{P}}_{t-1} = \{\tilde{\mathbf{p}}_1, \tilde{\mathbf{p}}_2, \dots, \tilde{\mathbf{p}}_{t-1}\}$ are corresponding to the discrete grid points in \mathcal{X} . Based on the estimated locations in the past κ time slots, the mean velocity $\bar{\mathbf{v}}$ is calculated as $\bar{\mathbf{v}} = (\tilde{\mathbf{p}}_{t-1} - \tilde{\mathbf{p}}_{t-\kappa-1}) / (\kappa \delta_t)$ where δ_t is the time slot.

Consequently, the truncated location transition model can be established as

$$\begin{aligned} & \mathbb{P}(\mathbf{p}_t = \mathbf{x}_j | \mathbf{p}_{t-1} = \mathbf{x}_i) \\ & \propto \begin{cases} \exp(-\|\mathbf{x}_j - (\mathbf{x}_i + \delta_t \bar{\mathbf{v}})\|_2^2) & \text{if } \|\mathbf{x}_j - \mathbf{x}_i\|_2^2 \leq D_m \\ 0 & \text{otherwise.} \end{cases} \quad (15) \end{aligned}$$

where D_m is a predetermined constant to evaluate whether \mathbf{x}_j is reachable from \mathbf{x}_i in one time slot δ_t .

The trajectory discovery problem in (13) can be solved by a recursive algorithm as shown in Algorithm 1. The main idea is to establish a matrix $\mathbf{P} \in \mathbb{R}^{N \times T}$ recording the cumulative log-likelihood for the past observations given each possible trajectory, and a matrix \mathbf{Q} recording all the possible trajectories. The time complexity of Algorithm 1 is $O(TN^2)$, and the space complexity is $O(TN)$.

Algorithm 1 Trajectory Discovery with a Recursive Strategy

Input: Radio maps $\mathcal{M}^{(q)}$, observations $\mathcal{Y}_T^{(q)}$ for $q \in \mathcal{Q}$, a time slot δ_T , variances σ_h^2 and σ_n^2 , and an initial probability \mathbb{P}_0 .

- 1) Initialize a probability matrix $\mathbf{P} \in \mathbb{R}^{N \times T}$ and a pointer matrix $\mathbf{Q} \in \mathbb{R}^{N \times T}$. Denote $P_{i,t}$ and $Q_{i,t}$ as the element of the i th row and t -column of \mathbf{P} and \mathbf{Q} , respectively. Initialize a trajectory index vector $\boldsymbol{\tau} = [\tau_1, \tau_2, \dots, \tau_T]$.
- 2) Initialize \mathbf{P} and \mathbf{Q} at $t = 1$:
 - a) For $i = 1, 2, \dots, N$:
 - i) Update $P_{i,1} \leftarrow \sum_{q \in \mathcal{Q}} \log p(\mathbf{y}_1^{(q)} | \mathbf{p}_1 = \mathbf{x}_i) + \log \mathbb{P}_0$, and $Q_{i,1} \leftarrow 0$.
- 3) Iteratively update \mathbf{P} and \mathbf{Q} from $t = 2$ to $i = T$:
 - a) For $t = 2, 3, \dots, T$:
 - i) For $i = 1, 2, \dots, N$:
 - A) Initialize $\mathcal{W} = \{w_1, w_2, \dots, w_N\}$.
 - B) Update $w_j \leftarrow P_{i,t-1} + \log \mathbb{P}(\mathbf{p}_t = \mathbf{x}_j | \mathbf{p}_{t-1} = \mathbf{x}_i) + \sum_{q=1}^Q \log p(\mathbf{y}_t^{(q)} | \mathbf{p}_t = \mathbf{x}_j)$ for $j = 1, 2, \dots, N$.
 - C) Update $P_{i,t} \leftarrow \max_{w_j \in \mathcal{W}} w_j$, and $Q_{i,t} = \arg\max_{j \in \{1, 2, \dots, N\}} w_j$.
- 4) Let $\tau_T \leftarrow \arg\max_{i \in \{1, 2, \dots, N\}} P_{i,T}$.
- 5) Recursively update $\tau_t \leftarrow Q_{\tau_{t+1}, t+1}$ for $t = T-1, T-2, \dots, 1$.
- 6) Output the estimated trajectory $\tilde{\mathcal{P}}_T = \{\mathbf{x}_{\tau_1}, \mathbf{x}_{\tau_2}, \dots, \mathbf{x}_{\tau_T}\}$.

C. Channel Estimation Under the Discovered Trajectory

To estimate the channel $\mathbf{h}_T^{(q)}$ at the current location \mathbf{p}_T in problem (11), one only needs to consider the current measurement $\mathbf{y}_T^{(q)}$ and the user location \mathbf{p}_T at time $t = T$. This is due to the fact that $\mathbf{y}_T^{(q)}$ only depends on the measurement location \mathbf{p}_T and is independent of $\mathcal{Y}_{T-1}^{(q)}$. Then, the objective function for channel estimation can be formulated as $p(\mathbf{y}_T^{(q)} | \mathbf{p}_T) = \int p(\mathbf{y}_T^{(q)} | \mathbf{h}, \mathbf{p}_T) d\mathbf{h} = \int p(\mathbf{y}_T^{(q)}, \mathbf{h} | \mathbf{p}_T) p(\mathbf{h} | \mathbf{p}_T) d\mathbf{h} = \int p(\mathbf{y}_T^{(q)} | \mathbf{h}) p(\mathbf{h} | \mathbf{p}_T) d\mathbf{h}$ because the real-time measurement $\mathbf{y}_T^{(q)}$ and the user location \mathbf{p}_T are conditionally independent given the hidden variable \mathbf{h} . Given $\mathbf{h}_T^{(q)}$ as the observed channel at \mathbf{p}_T , $p(\mathbf{h} | \mathbf{p}_T)$ can be approximated as a Delta function where the impulse appears at $\mathbf{h} = \mathbf{h}_T^{(q)}$. Therefore, $p(\mathbf{y}_T^{(q)} | \mathbf{p}_T)$ can be approximated by $p(\mathbf{y}_T^{(q)} | \mathbf{h}_T^{(q)}) p(\mathbf{h}_T^{(q)} | \mathbf{p}_T)$, and the log-likelihood of $p(\mathbf{y}_T^{(q)} | \mathbf{h}_T^{(q)}) p(\mathbf{h}_T^{(q)} | \mathbf{p}_T)$ is given by $\log p(\mathbf{y}_T^{(q)} | \mathbf{h}_T^{(q)}) + \log p(\mathbf{h}_T^{(q)} | \mathbf{p}_T)$.

Hence, the channel estimation problem for BS q can be extracted from problem (11), and formulated as

$$\underset{\mathbf{h}_T^{(q)}}{\text{maximize}} \quad \log p(\mathbf{y}_T^{(q)} | \mathbf{h}_T^{(q)}) + \log p(\mathbf{h}_T^{(q)} | \mathbf{p}_T) \quad (16)$$

Problem (16) has a closed-form solution $\tilde{\mathbf{h}}_T^{(q)}$ given the channel covariance $\mathbf{C}^{(q)}(\mathbf{p}_T)$ at the current position \mathbf{p}_T .

Theorem 1 (Optimal channel estimation). *The globally optimal solution to Problem (16) is given by*

$$\tilde{\mathbf{h}}_T^{(q)} = (\mathbf{A}^H \mathbf{A} + \sigma_n^2 (\mathbf{C}^{(q)}(\mathbf{p}_T) + \sigma_h^2 \mathbf{I}_{N_t \times N_t})^{-1})^{-1} \mathbf{A}^H \mathbf{y}_T^{(q)}. \quad (17)$$

Proof. See Appendix A. \square

Theorem 1 indicates that the channel estimation performance not only depends on the channel covariance at the current location, but also depends on the combining matrix \mathbf{A} . Next, the combining matrix \mathbf{A} is adaptively designed by exploring the subspace of the channel covariance such that the number of pilot is greatly reduced.

D. CSI Tracking with the Exploration of Channel Covariance Subspace

The number of observations is limited due to the high-speed movement of users or possibly long piloting period. To ensure a small number of observations can capture the main information of the MIMO channel, this section proposes a CSI tracking strategy with adaptive combining matrix. Specifically, the combining matrix \mathbf{A} is adaptively designed by exploring the subspace of the channel covariance at the current location. In particular, the observation model in (4) is rewritten as

$$\mathbf{y}_t^{(q)} = \mathbf{A}_t^{(q)} \mathbf{h}_t^{(q)} + \mathbf{n}_t^{(q)}. \quad (18)$$

where $\mathbf{A}_t^{(q)}$ is the combining matrix chosen for the q th BS at time t .

Denote the channel covariance at \mathbf{p}_t as $\tilde{\mathbf{C}}^{(q)}(\mathbf{p}_t) = \mathbf{C}^{(q)}(\mathbf{p}_t) + \sigma_h^2 \mathbf{I}_{N_t \times N_t}$ which consists of the deterministic channel covariance and the random channel covariance. To find a matrix $\mathbf{A}_t^{(q)} \in \mathbb{C}^{M \times N_t}$ such that the observation $\mathbf{y}_t^{(q)} = \mathbf{A}_t^{(q)} \mathbf{h}_t^{(q)}$ retains most of the energy of $\mathbf{h}_t^{(q)}$, the following observation energy maximization problem is formulated:

$$\begin{aligned} & \underset{\mathbf{A}_t^{(q)}}{\text{maximize}} \quad \mathbb{V}\{\mathbf{A}_t^{(q)} \mathbf{h}_t^{(q)}\} \\ & \text{subject to} \quad \mathbf{A}_t^{(q)} (\mathbf{A}_t^{(q)})^H = \mathbf{I}_{M \times M} \\ & \quad \mathbb{E}\{\mathbf{h}_t^{(q)} (\mathbf{h}_t^{(q)})^H\} = \tilde{\mathbf{C}}^{(q)}(\mathbf{p}_t) \end{aligned} \quad (19)$$

where the constraint $\mathbf{A}_t^{(q)} (\mathbf{A}_t^{(q)})^H = \mathbf{I}_{M \times M}$ ensures that the columns of $\mathbf{A}_t^{(q)}$ are orthogonal to each other, and maintains the stable signal power, and the constraint $\mathbb{E}\{\mathbf{h}_t^{(q)} (\mathbf{h}_t^{(q)})^H\} = \tilde{\mathbf{C}}^{(q)}(\mathbf{p}_t)$ specifies that the statistical properties of the channel $\mathbf{h}_t^{(q)}$ adhere to the channel covariance $\tilde{\mathbf{C}}^{(q)}(\mathbf{p}_t)$. Problem (19) can be solved using the idea of Principal Component Analysis (PCA), and the closed-form solution of $\mathbf{A}_t^{(q)}$ is given by the following proposition.

Proposition 1 (Optimal probing matrices). *The solution to problem (19) is given by*

$$(\mathbf{A}_t^{(q)})^* = [\mathbf{u}_{t,1}^{(q)}, \mathbf{u}_{t,2}^{(q)}, \dots, \mathbf{u}_{t,M}^{(q)}]^H \quad (20)$$

where $\mathbf{u}_{t,m}^{(q)}$ is the eigenvector corresponding to the largest m th eigenvalue of $\tilde{\mathbf{C}}^{(q)}(\mathbf{p}_t)$.

Proof. See Appendix B. \square

Since the location \mathbf{p}_t is unknown before measuring, the channel covariance $\tilde{\mathbf{C}}^{(q)}(\mathbf{p}_t)$ is unavailable. Nevertheless, one can use the last estimated location $\tilde{\mathbf{p}}_{t-1} = \mathbf{x}_i$ from Algorithm 1, the mobility model (15), and the radio map \mathcal{M} to estimate the channel covariance at the current position \mathbf{p}_t . Specifically, the channel covariance at \mathbf{p}_t is estimated as the weighted average of the channel covariance around $\tilde{\mathbf{p}}_{t-1}$, i.e.,

$$\hat{\mathbf{C}}^{(q)}(\mathbf{p}_t) = \sum_{\mathbf{x}_j \in \mathcal{X}} \tilde{\mathbf{C}}_j^{(q)} \mathbb{P}(\mathbf{p}_t = \mathbf{x}_j | \tilde{\mathbf{p}}_{t-1} = \mathbf{x}_i). \quad (21)$$

However, if the combining matrix $(\mathbf{A}_t^{(q)})^*$ in (20) is utilized for measurement, the observation may lose some information such as path phases, and multi-path components, leading to large localization error. Consequently, the trajectory discovery method necessitates the random selection of channel components. Inspired by the subspace exploration of the deterministic channel covariance and the random feature extraction of the channel \mathbf{h}_t , the following strategy under $M = 1$ for joint trajectory discovery and channel estimation is proposed.

- **Random sampling stage:** For the first T_0 observations, use a Gaussian-distributed random combining matrix $\mathbf{A}_t^{(q)} \in \mathbb{C}^{1 \times N_t}$ to get the observation, i.e., $\mathbf{y}_t^{(q)} = \mathbf{A}_t^{(q)} \mathbf{h}_t^{(q)}(\mathbf{p}_t) \in \mathbb{C}^{1 \times 1}$, for $t \in \{1, 2, \dots, T_0\}$. Next, perform the trajectory discovery in Algorithm 1 and obtain the estimated location $\tilde{\mathbf{p}}_{T_0} \in \mathcal{G}_i$ and its corresponding channel covariance $\mathbf{C}_i^{(q)}$.
- **Refined CSI tracking stage:** From the measurement time $t = T_0 + 1$, the combining matrix $\mathbf{A}_t^{(q)} \in \mathbb{C}^{1 \times N_t}$ for the q th BS is chosen as the Hermitian of an eigenvector selected from the estimated channel covariance $\hat{\mathbf{C}}^{(q)}(\mathbf{p}_t)$ in (21). Denote the probability of selecting the m th eigenvector $\hat{\mathbf{u}}_{t,m}^{(q)}$ of the channel covariance $\hat{\mathbf{C}}^{(q)}(\mathbf{p}_t)$ as $\mathbb{P}(\hat{\mathbf{u}}_{t,m}^{(q)} | \hat{\mathbf{C}}^{(q)}(\mathbf{p}_t))$. Denote the m th eigenvalue of $\hat{\mathbf{C}}^{(q)}(\mathbf{p}_t)$ as $\hat{\lambda}_{t,m}^{(q)}$. Then, $\mathbb{P}(\hat{\mathbf{u}}_{t,m}^{(q)} | \hat{\mathbf{C}}^{(q)}(\mathbf{p}_t))$ is formulated as

$$\mathbb{P}(\hat{\mathbf{u}}_{t,m}^{(q)} | \hat{\mathbf{C}}^{(q)}(\mathbf{p}_t)) = \frac{\hat{\lambda}_{t,m}^{(q)}}{\sum_{m=1}^{N_t} \hat{\lambda}_{t,m}^{(q)}}. \quad (22)$$

, and thus, $\mathbf{A}_t^{(q)}$ is given by

$$\mathbf{A}_t^{(q)} = (\hat{\mathbf{u}}_{t,m}^{(q)})^H \text{ with probability } \mathbb{P}(\hat{\mathbf{u}}_{t,m}^{(q)} | \hat{\mathbf{C}}^{(q)}(\mathbf{p}_t)). \quad (23)$$

Then, the trajectory discovery is performed by maximizing $\log p(\mathbf{y}_t | \mathbf{p}_t)$ with the constraint $\mathbf{p}_t \in \mathcal{X}$ at each step, and the channel can be estimated at time $t = T$ using (17).

The probing matrix in (23) takes the advantages of both random exploration of channel and subspace exploitation of channel covariance. In addition, the observation number at each location is reduced to 1. The technical details are shown in Algorithm (2). The constant T_0 controls the length of the random exploration period. In particular, the case $T_0 = 1$ corresponds to the scenario that the CSI tracking is performed from the second measurement whose probing matrix is partially generated based on the channel covariance at the first estimated location. In this case, the user localization performance is weakened because of insufficient exploration

Algorithm 2 Single-dimension Observations Driven CSI Tracking with the Exploration of Channel Covariance Subspace

Input: Radio maps $\mathcal{M}^{(q)}$ for $q \in \mathcal{Q}$, a time slot δ_T , variances σ_h^2 and σ_n^2 , and an initial mobility probability \mathbb{P}_0 .

- 1) Initialize a probability matrix $\mathbf{P} \in \mathbb{R}^{N \times T}$ and a pointer matrix $\mathbf{Q} \in \mathbb{R}^{N \times T}$.
- 2) Initialization at $t = 1, 2, \dots, T_0$:
 - a) Generate $\mathbf{A}_1^{(q)} \in \mathbb{C}^{1 \times N_t}$ as a Gaussian random matrix, send pilots, and observe measurements $\mathbf{y}_t^{(q)}$.
 - b) Conduct Step 2 in Algorithm 1.
 - c) Let $\tau_1 \leftarrow \arg\max_{i \in \{1, 2, \dots, N\}} P_{i,1.7}$
- 3) For $t = T_0 + 1, \dots, T$
 - a) Generate $\mathbf{A}_t^{(q)} = (\hat{\mathbf{u}}_{t,m}^{(q)})^H$ with probability $\mathbb{P}(\hat{\mathbf{u}}_{t,m}^{(q)} | \hat{\mathbf{C}}^{(q)}(\mathbf{p}_t))$ in (22) where $\hat{\mathbf{C}}^{(q)}(\mathbf{p}_t)$ is computed in 21, and $\hat{\mathbf{u}}_{t,m}^{(q)}$ is the m th eigenvector of $\hat{\mathbf{C}}^{(q)}(\mathbf{p}_t)$.
 - b) Conduct Step 3(a)i in Algorithm 1.
 - c) Let $\tau_t \leftarrow \arg\max_{i \in \{1, 2, \dots, N\}} P_{i,t}$.
- 4) Iteratively update $\tau_t \leftarrow Q_{\tau_{t+1}, t+1}$ for $t = T - 1, T - 2, \dots, 1$.
- 5) Output the estimated trajectory $\tilde{\mathcal{P}}_T = \{\mathbf{x}_{\tau_1}, \mathbf{x}_{\tau_2}, \dots, \mathbf{x}_{\tau_T}\}$, and the estimated channel $(\mathbf{h}_T^{(q)})^*$ at $t = T$ using (17).

of the multipath components of the channel. On the other hand, the case $T_0 = T$ implies that there is no CSI tracking stage, which fails to capture the main information of the channel, resulting in poor channel estimation. The numerical results in Section (V) confirms the above statements.

IV. RADIO MAP CONSTRUCTION WITH UNCERTAIN LOCATIONS

A. Problem for Joint Radio Map Construction, Trajectory Discovery, and Channel Estimation

The low-overhead CSI tracking and precise channel estimation requires a channel covariance radio map \mathcal{M} defined in 6. However, the construction of \mathcal{M} desires adequate sampling of channels with their location information in the area of interest, which is of high cost, especially in a MIMO environment.

To jointly construct a radio map while performing trajectory discovery and channel estimation, problem (11) is reformulated as

$$\begin{aligned}
 & \underset{\mathcal{P}_T, \{\mathcal{M}^{(q)}\}_{q \in \mathcal{Q}, \mathcal{H}_Q}}{\text{maximize}} && \sum_{t=1}^T \sum_{q \in \mathcal{Q}} \log p(\mathbf{y}_t^{(q)} | \mathbf{p}_t, \mathbf{C}^{(q)}(\mathbf{p}_t)) \\
 & && + \sum_{t=2}^T \log \mathbb{P}(\mathbf{p}_t | \mathbf{p}_{t-1}) + \log \mathbb{P}(\mathbf{p}_1) \\
 & && + \mu \sum_{t=1}^T \|\mathbf{p}_t - \hat{\mathbf{p}}_t\|_2 / T \\
 & \text{subject to} && \mathbf{p}_t \in \mathcal{X} \\
 & && \|\mathbf{p}_t - \mathbf{p}_{t-1}\|_2 \leq D_m, \quad \forall t \in \{2, 3, \dots, T\}
 \end{aligned} \tag{24}$$

where μ is a penalizing factor to refine the trajectory discovery, and $\hat{\mathbf{p}}_t$ is a coarse location measured at time t . Note that the location error $\|\hat{\mathbf{p}}_t - \mathbf{p}_t\|_2$ could be tens of meters or even hundreds of meters, the proposed scheme still works well because the channel covariance map captures the channel distributions instead of the accurate channel information at certain locations.

B. Channel Covariance Map Construction

After obtaining the estimated trajectory $\tilde{\mathcal{P}}_T = \{\tilde{\mathbf{p}}_1, \tilde{\mathbf{p}}_2, \dots, \tilde{\mathbf{p}}_T\}$ using Algorithm 1, each observation $\mathbf{y}_t^{(q)} \in \mathcal{Y}_T^{(q)}$ is allocated to the measurement cluster denoted as $\tilde{\mathcal{Y}}_i^{(q)}$ according to $\tilde{\mathbf{p}}_t \in \mathcal{G}_i$. Given N grids in the area of interest, there are at most N measurement clusters $\tilde{\mathcal{Y}}_1^{(q)}, \tilde{\mathcal{Y}}_2^{(q)}, \dots, \tilde{\mathcal{Y}}_N^{(q)}$ centered at $\mathbf{x}_1, \mathbf{x}_2, \dots, \mathbf{x}_N$.

Based on the PDF of $p(\mathbf{y}_t^{(q)} | \mathbf{C}_i^{(q)})$ in (5), the PDF of $p(\tilde{\mathcal{Y}}_i^{(q)} | \mathbf{C}_i^{(q)})$ is given by

$$p(\tilde{\mathcal{Y}}_i^{(q)} | \mathbf{C}_i^{(q)}) = \prod_{\mathbf{y}_t^{(q)} \in \tilde{\mathcal{Y}}_i^{(q)}} p(\mathbf{y}_t^{(q)} | \mathbf{x}_i) = \prod_{\mathbf{y}_t^{(q)} \in \tilde{\mathcal{Y}}_i^{(q)}} p(\mathbf{y}_t^{(q)} | \mathbf{C}_i^{(q)}). \tag{25}$$

To construct the deterministic channel covariance for the q th BS, the log-likelihood of the posterior probability $p(\tilde{\mathcal{Y}}_i^{(q)} | \mathbf{C}_i^{(q)})$ is going to be maximized. Therefore, a channel covariance map construction problem can be extracted from problem (24) as

$$\underset{\mathcal{M}^{(q)}}{\text{maximize}} \sum_{i=1}^N \log p(\tilde{\mathcal{Y}}_i^{(q)} | \mathbf{C}_i^{(q)}) \tag{26}$$

where $\mathbf{C}_i^{(q)}$ for $i \in \mathcal{N}$ in $\mathcal{M}^{(q)}$ is the variable to be estimated.

Define a function $F(\{\mathbf{C}_i^{(q)}\}_{i \in \mathcal{N}})$ as $F(\{\mathbf{C}_i^{(q)}\}_{i \in \mathcal{N}}) \triangleq \sum_{i=1}^N \sum_{\mathbf{y}_t^{(q)} \in \tilde{\mathcal{Y}}_i^{(q)}} \frac{1}{|\tilde{\mathcal{Y}}_i^{(q)}|} \log p(\mathbf{y}_t^{(q)} | \mathbf{C}_i^{(q)})$. It is easy to verify that maximizing $\sum_{i=1}^N \log p(\tilde{\mathcal{Y}}_i^{(q)} | \mathbf{C}_i^{(q)})$ in problem (26) is equivalent to maximizing $F(\{\mathbf{C}_i^{(q)}\}_{i \in \mathcal{N}})$. Therefore, problem (26) can be equivalently rewritten as

$$\underset{\{\mathbf{C}_i^{(q)}\}_{i \in \mathcal{N}}}{\text{maximize}} F(\{\mathbf{C}_i^{(q)}\}_{i \in \mathcal{N}}). \tag{27}$$

Problem (27) can be solved by exploiting the subspace of the distributions of measurement samples. Denote the *average sampling covariance* for the i th clustered set $\tilde{\mathcal{Y}}_i^{(q)}$ as $\mathbf{M}_i^{(q)}$, i.e.,

$$\mathbf{M}_i^{(q)} = \frac{1}{|\tilde{\mathcal{Y}}_i^{(q)}|} \sum_{\mathbf{y}_t^{(q)} \in \tilde{\mathcal{Y}}_i^{(q)}} \mathbf{y}_t^{(q)} (\mathbf{y}_t^{(q)})^H. \tag{28}$$

The deterministic channel covariance $\mathbf{C}_i^{(q)}$ corresponding to the i th grid can be decomposed as $\mathbf{C}_i^{(q)} = \mathbf{U}_i^{(q)} \mathbf{\Sigma}_i^{(q)} (\mathbf{U}_i^{(q)})^H$ in which, $\mathbf{\Sigma}_i^{(q)}$ is a diagonal matrix whose diagonal elements being eigenvalues of $\mathbf{C}_i^{(q)}$, and $\mathbf{U}_i^{(q)}$ is a unitary matrix with columns corresponding to the eigenvectors of $\mathbf{C}_i^{(q)}$. The following proposition offers the relationship between the average sampling covariance and the subspace of the deterministic channel covariance.

Proposition 2 (Channel covariance estimation from sampling covariance). *Let \mathbf{A} be $\mathbf{A} = [\tilde{\mathbf{A}}, \mathbf{0}] \in \mathbb{R}^{M \times N_t}$ where $\tilde{\mathbf{A}} \in \mathbb{R}^{M \times M}$ is a unitary matrix. The critical point of $F(\{\mathbf{C}_i^{(q)}\}_{i \in \mathcal{N}})$ with $\mathbf{C}_i^{(q)} = \mathbf{U}_i^{(q)} \boldsymbol{\Sigma}_i^{(q)} (\mathbf{U}_i^{(q)})^H$ satisfies the following condition:*

$$\mathbf{M}_i^{(q)} (\mathbf{A} \mathbf{U}_i^{(q)}) = (\mathbf{A} \mathbf{U}_i^{(q)}) (\boldsymbol{\Sigma}_i^{(q)} \mathbf{P}_M + \sigma^2 \mathbf{P}_M) \quad (29)$$

where \mathbf{P}_M is given by $\mathbf{P}_M \triangleq (\mathbf{U}_i^{(q)})^H \mathbf{A}^H \mathbf{A} \mathbf{U}_i^{(q)}$.

Proof. See Appendix C. \square

The condition (29) in Proposition 2 implies that the channel covariance reconstruction problem can be transformed to an eigenvalue decomposition problem. Specifically, $\mathbf{A} \mathbf{U}_i^{(q)}$ and $\boldsymbol{\Sigma}_i^{(q)} \mathbf{P}_M + \sigma^2 \mathbf{P}_M$ can be constructed as collections of eigenvectors and eigenvalues of the average sampling covariance matrix $\mathbf{M}_i^{(q)}$, respectively. Denote the m th eigenvalue of $\mathbf{M}_i^{(q)}$ as $\bar{\lambda}_{i,m}^{(q)}$ with the corresponding eigenvector denoted as $\bar{\mathbf{u}}_{i,m}^{(q)}$. It follows that

$$\mathbf{M}_i^{(q)} \bar{\mathbf{u}}_{i,m}^{(q)} = \bar{\lambda}_{i,m}^{(q)} \bar{\mathbf{u}}_{i,m}^{(q)}. \quad (30)$$

To ensure that the eigenvalues in $\boldsymbol{\Sigma}_i^{(q)}$ is non-negative, the eigenvalues of \mathbf{M}_i satisfying $\bar{\lambda}_{i,m}^{(q)} - \sigma^2 \geq 0$ are chosen to reconstruct $\boldsymbol{\Sigma}_i^{(q)}$ and $\mathbf{U}_i^{(q)}$. Denote $\mathbf{A}^\dagger \in \mathbb{C}^{N_t \times M}$ as the Moore-Penrose pseudo inverse of \mathbf{A} . Then, $\mathbf{U}_i^{(q)}$ and $\boldsymbol{\Sigma}_i^{(q)}$ are estimated as $\mathbf{A}^\dagger \bar{\mathbf{U}}_i^{(q)}$ and $\boldsymbol{\Lambda}_i$, respectively where $\bar{\mathbf{U}}_i^{(q)} = [\bar{\mathbf{u}}_{i,1}^{(q)}, \bar{\mathbf{u}}_{i,2}^{(q)}, \dots, \bar{\mathbf{u}}_{i,M^*}^{(q)}, 0, \dots, 0] \in \mathbb{C}^{M \times N_t}$, and $\boldsymbol{\Lambda}_i = \text{diag}\{\bar{\lambda}_{i,1}^{(q)} - \sigma^2, \bar{\lambda}_{i,2}^{(q)} - \sigma^2, \dots, \bar{\lambda}_{i,M^*}^{(q)} - \sigma^2, 0, \dots, 0\} \in \mathbb{C}^{N_t \times N_t}$, in which $\bar{\lambda}_{i,m}^{(q)} - \sigma^2 \geq 0$ for $\forall m \in \{1, 2, \dots, M^*\}$.

Therefore, the estimated channel covariance $\tilde{\mathbf{C}}_i^{(q)}$ for $i \in \mathcal{N}$ and $q \in \mathcal{Q}$ is obtained as

$$\tilde{\mathbf{C}}_i^{(q)} = (\mathbf{A}^\dagger \bar{\mathbf{U}}_i^{(q)}) \boldsymbol{\Lambda}_i (\mathbf{A}^\dagger \bar{\mathbf{U}}_i^{(q)})^H. \quad (31)$$

C. Reduced Pilots and Batch Processing for Channel Tracking

In particular, if there is limited time for channel observation, the dimension M of the combining matrix \mathbf{A} is quite small compared with the number of antenna arrays N_t , and thus, the exploitation of the subspace of measurement samples in (30) is not sufficient, especially when $M = 1$, and the sampling covariance $\mathbf{M}_i^{(q)} \in \mathbb{C}^{1 \times 1}$.

To address this issue, a batch processing strategy for sequential CSI data is proposed. Specifically, a batch of \tilde{T} observations are grouped as a batch observation

$$\tilde{\mathbf{y}}_t^{(q)} = [(\mathbf{y}_{t-\tilde{T}+1}^{(q)})^T, (\mathbf{y}_{t-\tilde{T}+2}^{(q)})^T, \dots, (\mathbf{y}_t^{(q)})^T]^T \in \mathbb{C}^{\tilde{T} \times 1} \quad (32)$$

where \tilde{T} is the batch size of the virtual observation. Even though $M \ll N_t$, one can always choose a proper batch size to exploit the channel distributions.

Define a batch combining matrix as a group of combining matrix in the past \tilde{T} time slots, i.e.,

$$\tilde{\mathbf{A}} = [\mathbf{A}_{t-\tilde{T}+1}^T, \mathbf{A}_{t-\tilde{T}+2}^T, \dots, \mathbf{A}_t^T]^T \in \mathbb{C}^{\tilde{T} \times N_t} \quad (33)$$

where $\mathbf{A}_t \in \mathbb{C}^{M \times N_t}$ is the combining matrix at time t .

Next, the channel covariance estimation strategy proposed in Section IV-B works by substituting the observation \mathbf{y}_t for

Algorithm 3 Joint Radio Map Construction, Trajectory Discovery, and Channel Estimation with Uncertain Location

Input: historical observations $\{\hat{\mathbf{p}}_t, \mathbf{y}_t\}_{t=1,2,\dots,T_{\text{ini}}}$, a time slot δ_T , variances σ_h^2 and σ_n^2 , an initial mobility probability \mathbb{P}_0 , and a threshold δ_e .

- 1) Initialize the radio map $\mathcal{M}^{(q)}$ using historical observations $\{\hat{\mathbf{p}}_t, \mathbf{y}_t^{(q)}\}_{t=1,2,\dots,T_{\text{ini}}}$ based on (31).
- 2) Initialize a trajectory set $\tilde{\mathcal{P}}_t^{(i)} = \{\hat{\mathbf{p}}_t\}_{t=1,2,\dots,T_{\text{ini}}}$.
- 3) Set the iteration timer $i = 0$.
- 4) While $\|\tilde{\mathbf{p}}_t^{(i)} - \tilde{\mathbf{p}}_t^{(i-1)}\|_2 < \delta_e$
 - a) Get the current coarse location $\hat{\mathbf{p}}_t$, and add $\hat{\mathbf{p}}_t$ to the historical trajectory set $\tilde{\mathcal{P}}_t^{(i)}$.
 - b) Send pilots and group the observations as a batch observation $\tilde{\mathbf{y}}_t^{(q)}$ every \tilde{T} time slots using (32).
 - c) Estimate the channel covariance $\{\mathbf{C}_i^{(q)}\}_{i \in \mathcal{N}}$ using (31) by substituting $\mathbf{y}_t^{(q)}$ for the batch observation $\tilde{\mathbf{y}}_t^{(q)}$ in (28) and \mathbf{A} for the batch combining matrix $\tilde{\mathbf{A}}$ in (31).
 - d) Update $i \leftarrow i + 1$.
 - e) Update the trajectory $\tilde{\mathcal{P}}_t^{(i)}$ according to Algorithm 1.
- 5) Estimate the channels $\mathbf{h}_T^{(q)}$ for $q \in \mathcal{Q}$ using (17).
- 6) Output the estimated channel $\tilde{\mathbf{h}}_T^{(q)}$ for $q \in \mathcal{Q}$, the discovered trajectory $\tilde{\mathcal{P}}_T^{(i)}$, and the radio map $\mathcal{M}^{(q)}$ based on $\tilde{\mathcal{P}}_T^{(i)}$ and $\{\tilde{\mathbf{C}}_i^{(q)}\}_{i \in \mathcal{N}}$.

the batch observation $\tilde{\mathbf{y}}_t$ in (28) and the combining matrix \mathbf{A} for the batch combining matrix $\tilde{\mathbf{A}}$ in (31). This works because the channel covariances are similar to each other at locations in close proximity because they share the similar propagation environment, scattering and shadowing.

The technical details are shown in Algorithm (3). Note that the first iteration for channel covariance estimation requires a coarse user location while the initialized user locations do not need to be accurate, because the proposed scheme can group the locations according to the observations and the channel distributions.

V. NUMERICAL RESULTS

In this section, we present the experimental findings conducted on real city maps with 3D ray-tracing techniques for generating the channel database.

A. Environment Setup and Scenarios

The experiments are conducted on a MIMO CSI database generated by Wireless Insite[®] which provides 3D ray-tracing for the analysis of site-specific radio wave propagation and wireless communication systems. Specifically, the city topology is a 710 meters \times 740 meters area from San Francisco, America. The buildings' height ranges from 12 meters to 204 meters. We manually deploy 7 BSs on the top of some buildings for serving the area of interest as shown in Fig. 2(a). The MIMO antenna of each BS consists of $N_t = 64$ antenna arrays as shown in Fig. 2(b). The users are randomly dropped in the non-building area.

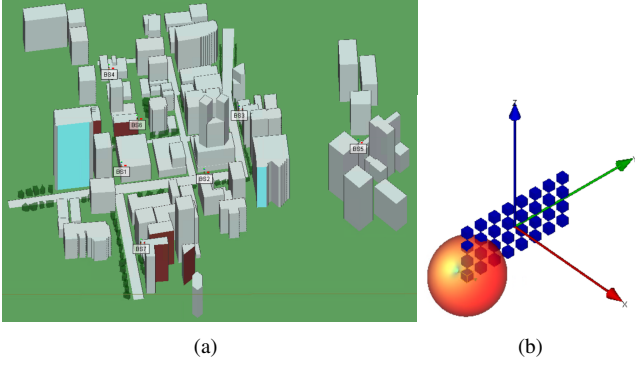


Figure 2. (a) Simulation environment where there are 7 BSs equipped with 32 dual-dipole MIMO antennas. (b) MIMO antennas with $N_t = 64$ antenna arrays.

By simulating random walk along roads in the map, the radio database is established and it contains 20269 user locations with its related CSI information. The user trajectories are randomly generated on the street. The observation $\mathbf{y}_t^{(q)}$ at each location \mathbf{p}_t is generated using (4) where the actual channel $\mathbf{h}_t^{(q)}$ is generated using the ray-tracing technique of Wireless Insite[®]. To depict the uncertainty of locations, a random location shift following a Gaussian distribution $\mathcal{N}(0, 400)$ is added to the actual user location \mathbf{p}_t . The grid length of the radio map is 5 meters, the user velocity is set as 50 kilometer per hour (km/h), and the sampling period of each observation is 50 milliseconds. The batch size \tilde{T} is set as 20.

The following baseline schemes are compared with the proposed blind radio map construction and CSI tracking algorithm.

- AR-based channel estimation: This approach estimates the AR coefficients of the channel making use of measurements over the time and spatial dimensions. Then, the channel at time $t = T$ is estimated using the following AR model

$$\mathbf{h}_T^{(q)} = \Phi_1 \mathbf{h}_{T-1}^{(q)} + \dots + \Phi_{T-1} \mathbf{h}_1^{(q)} + \mathbf{w}(T) \quad (34)$$

where the matrices $\Phi_t = \alpha_t \mathbf{I}_{N_t \times N_t}$ for $t \in \{1, 2, \dots, T-1\}$ are assumed to be constant in time, and $\mathbf{w}(T) = [w_1(T), w_2(T), \dots, w_{N_t}(T)] \in \mathbb{C}^{N_t \times 1}$ is the white noise following a Gaussian distribution, i.e., $w_n(t) \sim \mathcal{CN}(0, \sigma_h^2)$ for $n \in \{1, 2, \dots, N\}$. Since the observation \mathbf{y}_t is collected at time t , we use the least squares (LS) channel estimation to derive \mathbf{h}_t using \mathbf{y}_t , i.e., $\mathbf{h}_t = (\mathbf{A}^H \mathbf{A})^{-1} \mathbf{A}^H \mathbf{y}_t$. In practice, it is difficult to obtain the full observation of the channel, i.e., $M = N_t$, we randomly generated the combining matrix $\mathbf{A} \in \mathbb{C}^{(N_t/2) \times N_t}$ for observation collection.

- LSTM-based channel estimation: This scheme utilizes the advantages of LSTM in processing time sequences. The applied LSTM is an improved recurrent neural network (RNN) algorithm by adding structure including cell states. Specifically, the previous $p-1$ observations are used to train the network, and the input of the LSTM neural network is $\{\mathbf{h}_1^{(q)}, \mathbf{h}_2^{(q)}, \dots, \mathbf{h}_{p-1}^{(q)}\}$. The output of the network is $\bar{\mathbf{h}}_p$ at time $t = p$, which is the estimated

value of \mathbf{h}_p . Similar to the AR-based channel predictor, we randomly generate $\mathbf{A} \in \mathbb{C}^{(N_t/2) \times N_t}$ for observation collection, and use the LS channel estimation to derive \mathbf{h}_t based on the observation $\mathbf{y}_t \in \mathbb{C}^{N_t \times 1}$.

- Perfect radio map-assisted CSI tracking and channel estimation: This scheme utilizes all the data of channels and perfect location information to construct the radio map $\mathcal{M}^{(q)}$ for $q \in \mathcal{Q}$. Based on the constructed radio map, we perform the trajectory discovery using Algorithm 1, and estimates the channel based on the derived solution (17).

To evaluate the performance of the proposed schemes, the following criteria is defined.

- Localization error: Given the actual user trajectory $\mathcal{P}_t = \{\mathbf{p}_1, \mathbf{p}_2, \dots, \mathbf{p}_t\}$ and the discovered user trajectory $\tilde{\mathcal{P}}_T = \{\mathbf{x}_{\tau_1}, \mathbf{x}_{\tau_2}, \dots, \mathbf{x}_{\tau_T}\}$ of Algorithm 1, the localization error is defined as

$$L(\mathcal{P}_t, \tilde{\mathcal{P}}_T) = \frac{\sum_{t=1}^T \|\mathbf{p}_t - \mathbf{x}_{\tau_t}\|_2}{T}.$$

- Channel capacity efficiency ratio: Based on the maximum ratio combining (MRC) for a single-user MIMO system, the channel capacity is calculated as $f(\tilde{\mathbf{h}}, \mathbf{h}) = \log_2(1 + |\tilde{\mathbf{h}}^H \mathbf{h}| / \sigma_n^2)$ where $\tilde{\mathbf{h}}$ is the estimated channel and \mathbf{h} is the actual channel. Given the estimated channel $\tilde{\mathbf{h}}_T^{(q)}$ and the perfect channel $\mathbf{h}_T^{(q)}$ for $q \in \mathcal{Q}$ at time $t = T$, the channel capacity efficiency ratio is defined as

$$E_T = \max_{q \in \mathcal{Q}} \frac{f(\tilde{\mathbf{h}}_T^{(q)}, \mathbf{h}_T^{(q)})}{f(\mathbf{h}_T^{(q)}, \mathbf{h}_T^{(q)})}.$$

- Normalized channel covariance error: To evaluate the performance of the construction of future work will focus on xxx, which could further enhance the practical implementation and scalability of the proposed framework. Additionally, xxx could be explored to further optimize the performance of CSI tracking in larger-scale, real-world networks. the channel covariance map, we define the following normalized channel covariance error. Define the perfect channel covariance in the i th grid as $\mathbf{C}_i^{(q)}$ which is constructed using all the deterministic channels in the i th grid from the dataset. Given the estimated channel covariance $\tilde{\mathbf{C}}_i^{(q)}$ and the perfect channel covariance $\mathbf{C}_i^{(q)}$ in the i th grid, the normalized channel covariance error is defined as $\sum_{i \in \mathcal{N}} \|\mathbf{C}_i^{(q)} / \|\mathbf{C}_i^{(q)}\|_{\text{fro}} - \tilde{\mathbf{C}}_i^{(q)} / \|\tilde{\mathbf{C}}_i^{(q)}\|_{\text{fro}}\|_{\text{fro}} / N$.

B. Radio Map-assisted Trajectory Discovery and Channel Estimation

With the assistance of radio map $\mathcal{M}^{(q)}$, fig. 3 and fig. 4 illustrate channel capacity efficiency ratio versus SNR. The number of observations is 400, which corresponds to about 280 meters as the velocity is 50 km/h and the observations are collected every 50 ms. It is found that the if all the channel data are utilized to construct the radio map, the radio map-assisted approach can achieve over 94% performance of the perfect channel when SNR is equal to or greater than 10 dB. The proposed Algorithm 3 utilizes 1800 historical observations to initialize a radio map, and then it also achieves

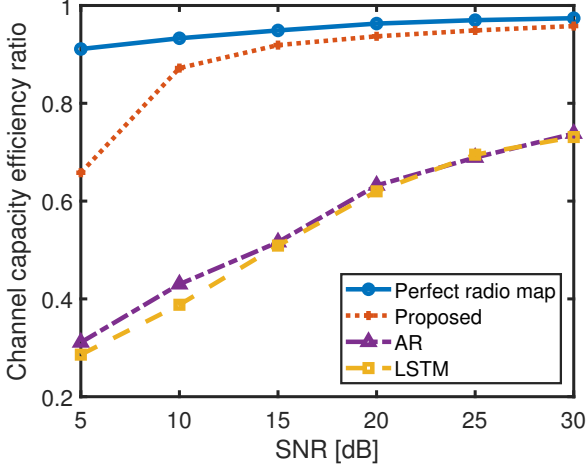


Figure 3. Channel capacity efficiency ratio versus SNR under 3 LOS BSs.

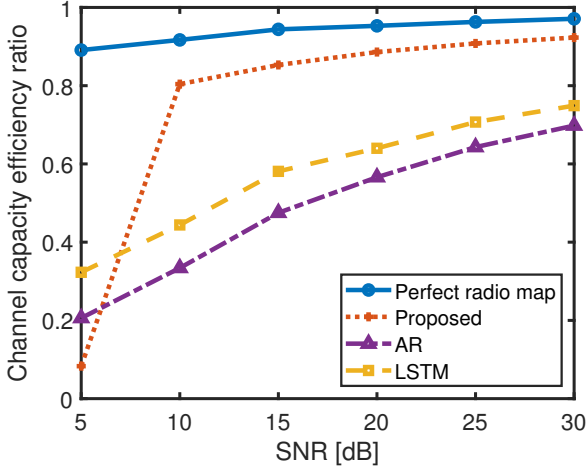


Figure 4. Channel capacity efficiency ratio versus SNR under 3 NLOS BSs.

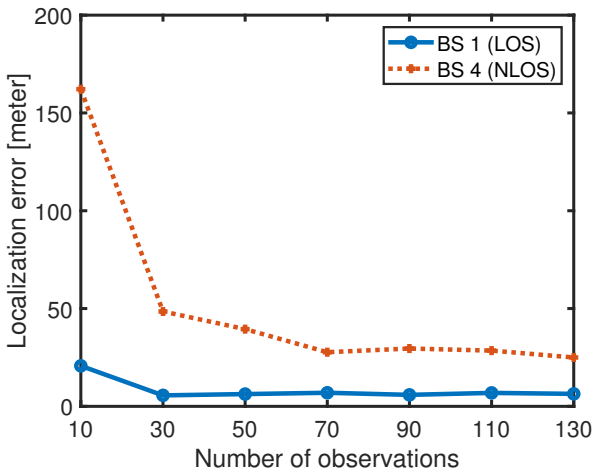


Figure 5. Localization error versus number of observations and type of BSs.

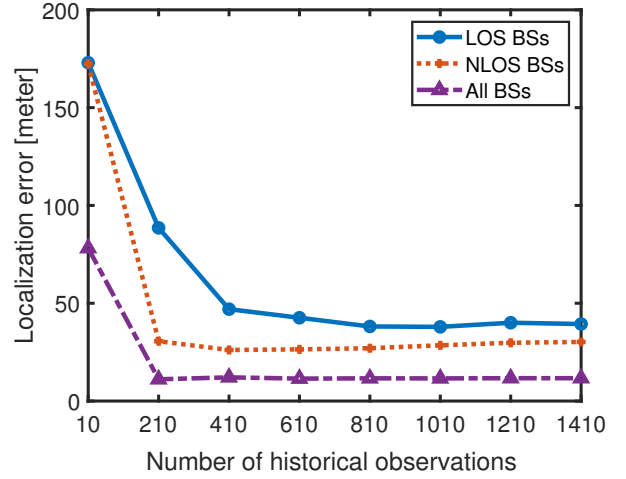


Figure 6. Localization error versus number of historical observations used for initializing the radio map.

over 90% channel capacity of that of perfect CSI. The AR and the LSTM approaches shows poor performance because they assume that the channel can be accurately represented with historical channels as shown in (34), and the performance of these approaches depend on the accuracy of estimation of historical channels.

Additionally, it is observed from fig. 3 and fig. 4 that the proposed radio map-assisted approach can also estimate the NLOS channels in an actual city environment. Although there are lots of scatters and reflections due to complex topological features, the radio map-assisted approach can still achieve over 94% performance of the perfect channel under SNR= 20 dB. The results from that the radio map has captured the deterministic channel distributions in presence of blockage.

Fig. 5 shows the localization error versus number of observations. The user trajectories are randomly generated, and they are LOS to BS 1 while NLOS to BS4. It is found that the radio-map assisted approach has a localization error of less than 5 meters when 30 observations are collected if the user trajectory is LOS to a BS. For user trajectories in NLOS conditions, the localization error can still be less than 30 meters when 70 observations are collected.

C. Radio Map Construction, Trajectory Discovery and Channel Estimation

Fig.6 shows the localization error versus the number of historical observations for initializing the radio map. It is found that more historical observations contribute to smaller localization error in the initial stage. Additionally, it is observed that more BSs perform better user localization. Fig.7 displays the channel capacity efficiency ratio versus the number of historical observations. User trajectories in LOS propagation conditions can obtain better channel estimation performance while it is more difficult to estimate MIMO channels in NLOS conditions. Fig.8 shows the localization error versus sampling period. It is found that the even the BS can collect observations with a higher rate, the sampling rate does not affect the

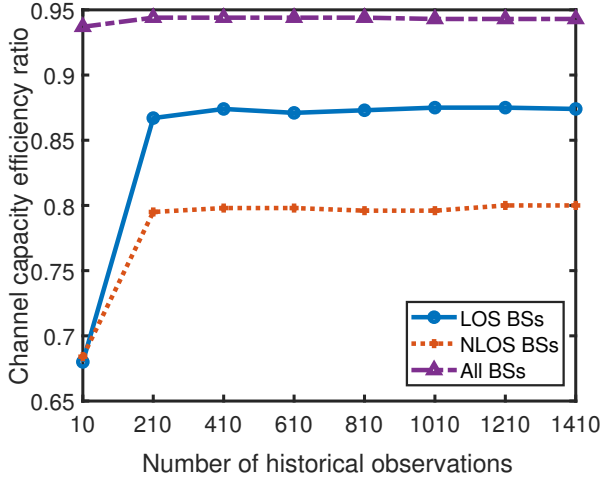


Figure 7. Channel capacity efficiency ratio versus number of historical observations used for initializing the radio map.

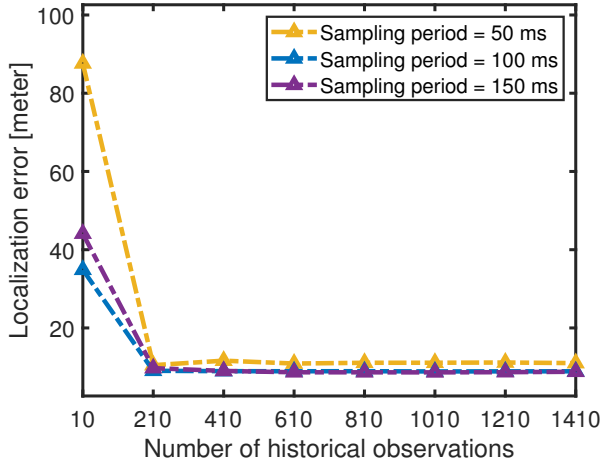


Figure 8. Localization error versus sampling period of each observation.

localization performance too much when there are enough historical observations for radio map construction.

VI. CONCLUSION

This paper presented a framework for radio map-assisted CSI tracking and trajectory discovery in massive MIMO networks, particularly suited for dynamic and dense urban environments. By redefining the radio map as a mapping from spatial positions to deterministic channel covariance matrices, we were able to effectively capture the spatially dependent nature of wireless channels. A CSI tracking method that leverages these channel covariance maps was proposed, enabling accurate CSI estimation using only single-dimensional observations at each location during user movement. Additionally, we proposed a coarse location-based radio map construction algorithm that refines the map online using sparse and sequential observations. Through extensive numerical experiments based on real city maps and ray-tracing MIMO channel datasets, it is demonstrated that the proposed framework

achieves superior performance in terms of both accuracy and adaptability compared to baseline methods.

APPENDIX A PROOF OF THEOREM 1

According to the observation model in (4), the PDF of $p(\mathbf{y}_T^{(q)}|\mathbf{h}_T^{(q)})$ is given by

$$p(\mathbf{y}_T^{(q)}|\mathbf{h}_T^{(q)}) = \frac{\exp(-(\mathbf{y}_T^{(q)} - \mathbf{A}\mathbf{h}_T^{(q)})^H(\mathbf{y}_T^{(q)} - \mathbf{A}\mathbf{h}_T^{(q)})/(2\sigma_n^2))}{(2\pi)^{M/2}\sigma_n} \quad (35)$$

Therefore, the log-likelihood of $p(\mathbf{y}_T^{(q)}|\mathbf{h}_T^{(q)})$ satisfies

$$\log p(\mathbf{y}_T^{(q)}|\mathbf{h}_T^{(q)}) \propto -\frac{\|\mathbf{y}_T^{(q)} - \mathbf{A}\mathbf{h}_T^{(q)}\|_2^2}{\sigma_n^2}. \quad (36)$$

In addition, since the channel $\mathbf{h}_T^{(q)}$ follows a complex Gaussian distribution in (3), and the deterministic channel covariance $\mathbf{C}^{(q)}(\mathbf{p}_T)$ is only dependent on the user location \mathbf{p}_T , the PDF of $p(\mathbf{h}_T^{(q)}|\mathbf{p}_T)$ is given by

$$p(\mathbf{h}_T^{(q)}|\mathbf{p}_T) = \frac{\exp(-(\mathbf{h}_T^{(q)})^H(\mathbf{C}^{(q)}(\mathbf{p}_T) + \sigma_h^2\mathbf{I}_{N_t \times N_t})^{-1}\mathbf{h}_T^{(q)}/2)}{(2\pi)^{N_t/2}|\mathbf{C}^{(q)}(\mathbf{p}_T) + \sigma_h^2\mathbf{I}_{N_t \times N_t}|^{1/2}} \quad (37)$$

It follows that

$$\log p(\mathbf{h}_T^{(q)}|\mathbf{p}_T) \propto -(\mathbf{h}_T^{(q)})^H(\mathbf{C}^{(q)}(\mathbf{p}_T) + \sigma_h^2\mathbf{I}_{N_t \times N_t})^{-1}\mathbf{h}_T^{(q)}. \quad (38)$$

Given (38) and (36), the log-likelihood of $p(\mathbf{y}_T^{(q)}|\mathbf{p}_T)$ satisfies that

$$\begin{aligned} \log p(\mathbf{y}_T^{(q)}|\mathbf{p}_T) \\ \propto -\frac{\|\mathbf{y}_T^{(q)} - \mathbf{A}\mathbf{h}_T^{(q)}\|_2^2}{\sigma_n^2} - (\mathbf{h}_T^{(q)})^H(\mathbf{C}^{(q)}(\mathbf{p}_T) + \sigma_h^2\mathbf{I}_{N_t \times N_t})^{-1}\mathbf{h}_T^{(q)}. \end{aligned} \quad (39)$$

Therefore, maximizing $\log p(\mathbf{y}_T^{(q)}|\mathbf{p}_T)$ is equivalent to maximizing $-\frac{\|\mathbf{y}_T^{(q)} - \mathbf{A}\mathbf{h}_T^{(q)}\|_2^2}{\sigma_n^2} - (\mathbf{h}_T^{(q)})^H(\mathbf{C}^{(q)}(\mathbf{p}_T) + \sigma_h^2\mathbf{I}_{N_t \times N_t})^{-1}\mathbf{h}_T^{(q)}$. Consequently, the problem (16) is equivalently rewritten as

$$\begin{aligned} \underset{\mathbf{h}_T^{(q)}}{\text{minimize}} \quad & \frac{\|\mathbf{y}_T^{(q)} - \mathbf{A}\mathbf{h}_T^{(q)}\|_2^2}{\sigma_n^2} \\ & + (\mathbf{h}_T^{(q)})^H(\mathbf{C}^{(q)}(\mathbf{p}_T) + \sigma_h^2\mathbf{I}_{N_t \times N_t})^{-1}\mathbf{h}_T^{(q)} \end{aligned} \quad (40)$$

The problem (40) is a convex problem because of the objective function is a summation of two quadratic-form functions. Let

$$\begin{aligned} H(\mathbf{h}_T^{(q)}) \triangleq & \frac{\|\mathbf{y}_T^{(q)} - \mathbf{A}\mathbf{h}_T^{(q)}\|_2^2}{\sigma_n^2} \\ & + (\mathbf{h}_T^{(q)})^H(\mathbf{C}^{(q)}(\mathbf{p}_T) + \sigma_h^2\mathbf{I}_{N_t \times N_t})^{-1}\mathbf{h}_T^{(q)}. \end{aligned} \quad (41)$$

The gradient of $H(\mathbf{h}_T^{(q)})$ is given by

$$\begin{aligned} \nabla_{\mathbf{h}_T^{(q)}} H(\mathbf{h}_T^{(q)}) = & -2\mathbf{A}^H(\mathbf{y}_T^{(q)} - \mathbf{A}\mathbf{h}_T^{(q)})/\sigma_n^2 \\ & + 2(\mathbf{C}^{(q)}(\mathbf{p}_T) + \sigma_h^2\mathbf{I}_{N_t \times N_t})^{-1}\mathbf{h}_T^{(q)}. \end{aligned} \quad (42)$$

Setting $\nabla_{\mathbf{h}_T^{(q)}} H(\mathbf{h}_T^{(q)})$ to 0, the globally optimal solution $\mathbf{h}_T^{(q)}$ to problem (16) and (40) is given by

$$\tilde{\mathbf{h}}_T^{(q)} = (\mathbf{A}^H \mathbf{A} + \sigma_n^2 (\mathbf{C}^{(q)}(\mathbf{p}_T) + \sigma_h^2 \mathbf{I}_{N_t \times N_t})^{-1})^{-1} \mathbf{A}^H \mathbf{y}_T^{(q)}. \quad (43)$$

APPENDIX B PROOF OF PROPOSITION (1)

The eigenvalue decomposition of $\tilde{\mathbf{C}}_i^{(q)} = \mathbf{C}_i^{(q)} + \sigma_h^2 \mathbf{I}_{N_t \times N_t}$ is given by

$$\begin{aligned} \tilde{\mathbf{C}}_i^{(q)} &= \mathbf{C}_i^{(q)} + \sigma_h^2 \mathbf{I}_{N_t \times N_t} \\ &= \mathbf{U}_i^{(q)} \boldsymbol{\Sigma}_i^{(q)} (\mathbf{U}_i^{(q)})^H + \sigma_h^2 \mathbf{U}_i^{(q)} (\mathbf{U}_i^{(q)})^H \\ &= \mathbf{U}_i^{(q)} (\boldsymbol{\Sigma}_i^{(q)} + \sigma_h^2 \mathbf{I}_{N_t \times N_t}) (\mathbf{U}_i^{(q)})^H. \end{aligned} \quad (44)$$

where $\boldsymbol{\Sigma}_i^{(q)} = \text{diag}\{\lambda_{i,1}^{(q)}, \lambda_{i,2}^{(q)}, \dots, \lambda_{i,M}^{(q)}\}$ in which, $\lambda_{i,m}^{(q)}$ is the eigenvalue of $\mathbf{C}_i^{(q)}$ with $\lambda_{i,1}^{(q)} \geq \lambda_{i,2}^{(q)} \geq \dots \geq \lambda_{i,M}^{(q)}$, and $\mathbf{U}_i^{(q)}$ is the matrix consisting of corresponding eigenvectors. Define $\mathbf{U}_{i,M}^{(q)}$ as the collection of the first M eigenvector of $\mathbf{C}_i^{(q)}$, i.e., $\mathbf{U}_{i,M}^{(q)} \triangleq [\mathbf{u}_{i,1}^{(q)}, \mathbf{u}_{i,2}^{(q)}, \dots, \mathbf{u}_{i,M}^{(q)}]^H$.

Given the optimal solution $\mathbf{A}_t^{(q)}$ in (20), the variance of $\mathbf{y}_t^{(q)}$ with $\mathbf{p}_t \in \mathcal{G}_i$ is given by

$$\begin{aligned} \mathbb{V}\{\mathbf{A}_t^{(q)} \mathbf{h}_t^{(q)}\} &= \mathbf{A}_t^{(q)} \tilde{\mathbf{C}}_i^{(q)} (\mathbf{A}_t^{(q)})^H \\ &= (\mathbf{U}_{i,M}^{(q)})^H \mathbf{U}_i^{(q)} (\boldsymbol{\Sigma}_i^{(q)} + \sigma_h^2 \mathbf{I}_{N_t \times N_t}) (\mathbf{U}_i^{(q)})^H \mathbf{U}_{i,M}^{(q)} \\ &\stackrel{(i)}{=} \tilde{\mathbf{I}}_{M \times N_t} (\boldsymbol{\Sigma}_i^{(q)} + \sigma_h^2 \mathbf{I}_{N_t \times N_t}) \tilde{\mathbf{I}}_{M \times N_t}^H \end{aligned} \quad (45)$$

where $\stackrel{(i)}{=}$ is because that $\mathbf{U}_i^{(q)}$ is an orthogonal matrix and $\tilde{\mathbf{I}}_{M \times N_t} = [\mathbf{I}_{M \times M}, \mathbf{0}_{M \times N_t}]$.

Therefore, $\mathbb{V}\{\mathbf{A}_t^{(q)} \mathbf{h}_t^{(q)}\}$ captures the largest M eigenvalues of $\tilde{\mathbf{C}}_i^{(q)}$, and thus, is maximized.

APPENDIX C PROOF OF PROPOSITION 2

Recall that $\mathbf{D}_i^{(q)} = \mathbf{A} \mathbf{C}_i^{(q)} \mathbf{A}^H + \sigma^2 \mathbf{I}_{M \times M}$ and $\mathbf{C}_i^{(q)} = \mathbf{U}_i^{(q)} \boldsymbol{\Sigma}_i^{(q)} (\mathbf{U}_i^{(q)})^H$. Define $\mathbf{V}_i^{(q)} \triangleq \mathbf{A} \mathbf{U}_i^{(q)} (\boldsymbol{\Sigma}_i^{(q)})^{1/2}$, and thus, $\mathbf{D}_i^{(q)}$ is rewritten as

$$\mathbf{D}_i^{(q)} = \mathbf{V}_i^{(q)} (\mathbf{V}_i^{(q)})^H + \sigma^2 \mathbf{I}_{M \times M}. \quad (46)$$

Setting the derivative of $F(\{\mathbf{C}_i^{(q)}\}_{i \in \mathcal{N}})$ with respect to (w.r.t.) $\mathbf{V}_i^{(q)}$ to 0, one can obtain

$$\frac{\partial F}{\partial \mathbf{V}_i^{(q)}} = (\mathbf{D}_i^{(q)})^{-1} \mathbf{M}_i^{(q)} (\mathbf{D}_i^{(q)})^{-1} \mathbf{V}_i^{(q)} - (\mathbf{D}_i^{(q)})^{-1} \mathbf{V}_i^{(q)} = 0 \quad (47)$$

where $\mathbf{M}_i^{(q)}$ is the average sampling covariance defined in (28).

Hence, the critical point of $F(\{\mathbf{C}_i^{(q)}\}_{i \in \mathcal{N}})$ w.r.t. $\mathbf{V}_i^{(q)}$ satisfies

$$\mathbf{M}_i^{(q)} (\mathbf{D}_i^{(q)})^{-1} \mathbf{V}_i^{(q)} = \mathbf{V}_i^{(q)}. \quad (48)$$

Since $(\mathbf{A} \mathbf{U}_i^{(q)}) (\mathbf{A} \mathbf{U}_i^{(q)})^H = \mathbf{A} \mathbf{U}_i^{(q)} (\mathbf{U}_i^{(q)})^H \mathbf{A}^H = \mathbf{I}_{M \times M}$, it follows that $\mathbf{A} \mathbf{U}_i^{(q)}$ is semi-unitary. Therefore, we have

$$\begin{aligned} (\mathbf{D}_i^{(q)})^{-1} \mathbf{V}_i^{(q)} &= \left(\mathbf{V}_i^{(q)} (\mathbf{V}_i^{(q)})^H + \sigma^2 \mathbf{I}_{M \times M} \right)^{-1} \mathbf{V}_i^{(q)} \\ &= \left(\mathbf{A} \mathbf{U}_i^{(q)} \tilde{\boldsymbol{\Sigma}}_i^{(q)} (\mathbf{U}_i^{(q)})^H \mathbf{A}^H \right)^{-1} \mathbf{V}_i^{(q)} \\ &= \left(\mathbf{A} \mathbf{U}_i^{(q)} \right) \left(\tilde{\boldsymbol{\Sigma}}_i^{(q)} \right)^{-1} \left(\mathbf{A} \mathbf{U}_i^{(q)} \right)^H \mathbf{V}_i^{(q)} \\ &= \mathbf{A} \mathbf{U}_i^{(q)} \left(\tilde{\boldsymbol{\Sigma}}_i^{(q)} \right)^{-1} \mathbf{P}_M (\boldsymbol{\Sigma}_i^{(q)})^{1/2} \\ &= \mathbf{V}_i^{(q)} (\tilde{\boldsymbol{\Sigma}}_i^{(q)})^{-1} \mathbf{P}_M \end{aligned} \quad (49)$$

where $\tilde{\boldsymbol{\Sigma}}_i^{(q)} = \boldsymbol{\Sigma}_i^{(q)} + \sigma^2 \mathbf{I}_{N_t \times N_t}$ and $\mathbf{P}_M = (\mathbf{U}_i^{(q)})^H \mathbf{A}^H \mathbf{A} \mathbf{U}_i^{(q)}$.

Given $\mathbf{A} = [\mathbf{A}, \mathbf{0}] \in \mathbb{R}^{M \times N_t}$ where $\bar{\mathbf{A}} \in \mathbb{R}^{M \times M}$ is a unitary matrix, we have

$$\mathbf{P}_M = (\mathbf{U}_i^{(q)})^H \mathbf{A}^H \mathbf{A} \mathbf{U}_i^{(q)} = \begin{bmatrix} \mathbf{I}_{M \times M} & \mathbf{0} \\ \mathbf{0} & \mathbf{0} \end{bmatrix}. \quad (51)$$

Substituting (51) into (49), it follows that $(\mathbf{D}_i^{(q)})^{-1} \mathbf{V}_i^{(q)} = \mathbf{V}_i^{(q)} (\boldsymbol{\Sigma}_i^{(q)} + \sigma^2 \mathbf{I}_{N_t \times N_t})^{-1} \mathbf{P}_M$, and thus, (48) can be simplified as

$$\mathbf{M}_i^{(q)} (\mathbf{A} \mathbf{U}_i^{(q)}) = (\mathbf{A} \mathbf{U}_i^{(q)}) (\boldsymbol{\Sigma}_i^{(q)} \mathbf{P}_M + \sigma^2 \mathbf{P}_M). \quad (52)$$

REFERENCES

- [1] R. Zhang, L. Cheng, S. Wang, Y. Lou, W. Wu, and D. W. K. Ng, "Tensor decomposition-based channel estimation for hybrid mmwave massive MIMO in high-mobility scenarios," *IEEE Trans. on Commun.*, vol. 70, no. 9, pp. 6325–6340, 2022.
- [2] Z. Wang, J. Zhang, H. Du, D. Niyato, S. Cui, B. Ai, M. Debbah, K. B. Letaief, and H. V. Poor, "A tutorial on extremely large-scale MIMO for 6G: Fundamentals, signal processing, and applications," *IEEE Commun. Surv. Tutorials*, vol. 26, no. 3, pp. 1560–1605, 2024.
- [3] M. Cui and L. Dai, "Channel estimation for extremely large-scale MIMO: Far-field or near-field?" *IEEE Trans. on Commun.*, vol. 70, no. 4, pp. 2663–2677, 2022.
- [4] O. Elijah, C. Y. Leow, T. A. Rahman, S. Nunoo, and S. Z. Iliya, "A comprehensive survey of pilot contamination in massive MIMO-5G system," *IEEE Commun. Surv. Tutorials*, vol. 18, no. 2, pp. 905–923, 2016.
- [5] C. Lin, J. Gao, R. Jin, and C. Zhong, "Self-adaptive measurement matrix design and channel estimation in time-varying hybrid mmwave massive MIMO-OFDM systems," *IEEE Trans. on Commun.*, vol. 72, no. 1, pp. 618–629, 2024.
- [6] J. Gao, M. Hu, C. Zhong, G. Y. Li, and Z. Zhang, "An attention-aided deep learning framework for massive MIMO channel estimation," *IEEE Trans. on Wireless Commun.*, vol. 21, no. 3, pp. 1823–1835, 2022.
- [7] I. M. Baby, K. Appaiah, and R. Chopra, "Optimal channel tracking and power allocation for time varying FDD massive MIMO systems," *IEEE Trans. on Commun.*, vol. 70, no. 2, pp. 1229–1244, 2022.
- [8] Y. Wan, G. Liu, A. Liu, and M.-J. Zhao, "Robust multi-user channel tracking scheme for 5G new radio," *IEEE Trans. on Wireless Commun.*, vol. 23, no. 6, pp. 5878–5894, 2024.
- [9] J. Vinogradova, G. Fodor, and P. Hammarberg, "On estimating the autoregressive coefficients of time-varying fading channels," in *Proc. IEEE Veh. Technol. Conf. (VTC)*, pp. 1–5, Helsinki, Finland, 2022.
- [10] Y. Wei, M.-M. Zhao, A. Liu, and M.-J. Zhao, "Channel tracking and prediction for IRS-aided wireless communications," *IEEE Trans. on Wireless Commun.*, vol. 22, no. 1, pp. 563–579, 2023.
- [11] Y. Zhao, X. Zhang, X. Gao, K. Yang, Z. Xiong, and Z. Han, "LSTM-based predictive mmwave beam tracking via sub-6 GHz channels for V2I communications," *IEEE Trans. on Commun.*, 2024, early access.
- [12] T. Peng, R. Zhang, X. Cheng, and L. Yang, "LSTM-based channel prediction for secure massive MIMO communications under imperfect CSI," in *Proc. IEEE Int. Conf. Commun. (ICC)*, pp. 1–6, Dublin, Ireland, 2020.

- [13] B. Zhou, X. Yang, S. Ma, F. Gao, and G. Yang, "Pay less but get more: A dual-attention-based channel estimation network for massive MIMO systems with low-density pilots," *IEEE Trans. on Wireless Commun.*, vol. 23, no. 6, pp. 6061–6076, 2024.
- [14] T.-K. Kim, Y.-S. Jeon, J. Li, N. Tavangaran, and H. V. Poor, "Semi-data-aided channel estimation for MIMO systems via reinforcement learning," *IEEE Trans. on Wireless Commun.*, vol. 22, no. 7, pp. 4565–4579, 2023.
- [15] A. Abdallah, A. Celik, M. M. Mansour, and A. M. Eltawil, "Deep learning-based frequency-selective channel estimation for hybrid mmwave MIMO systems," *IEEE Trans. on Wireless Commun.*, vol. 21, no. 6, pp. 3804–3821, 2022.
- [16] M. Arvinte and J. I. Tamir, "MIMO channel estimation using score-based generative models," *IEEE Trans. on Wireless Commun.*, vol. 22, no. 6, pp. 3698–3713, 2023.
- [17] Y. Teng, L. Jia, A. Liu, and V. K. N. Lau, "A hybrid pilot beamforming and channel tracking scheme for massive MIMO systems," *IEEE Trans. on Wireless Commun.*, vol. 20, no. 9, pp. 6078–6092, 2021.
- [18] Y. Han, S. Jin, C.-K. Wen, and X. Ma, "Channel estimation for extremely large-scale massive MIMO systems," *IEEE Commun. Lett.*, vol. 9, no. 5, pp. 633–637, 2020.
- [19] Y. Wang, X. Chen, Y. Cai, B. Champagne, and L. Hanzo, "Channel estimation for hybrid massive MIMO systems with adaptive-resolution ADCs," *IEEE Trans. on Commun.*, vol. 70, no. 3, pp. 2131–2146, 2022.
- [20] H. He, R. Wang, W. Jin, S. Jin, C.-K. Wen, and G. Y. Li, "Beamspace channel estimation for wideband millimeter-wave MIMO: A model-driven unsupervised learning approach," *IEEE Trans. on Wireless Commun.*, vol. 22, no. 3, pp. 1808–1822, 2023.
- [21] A. Zaib, M. Masood, A. Ali, W. Xu, and T. Y. Al-Naffouri, "Distributed channel estimation and pilot contamination analysis for massive MIMO-OFDM systems," *IEEE Trans. on Commun.*, vol. 64, no. 11, pp. 4607–4621, 2016.
- [22] Y. Ding, S.-E. Chiu, and B. D. Rao, "Bayesian channel estimation algorithms for massive MIMO systems with hybrid analog-digital processing and low-resolution ADCs," *IEEE J. Sel. Top. Signal Process.*, vol. 12, no. 3, pp. 499–513, 2018.
- [23] H. Kim, S. Kim, H. Lee, C. Jang, Y. Choi, and J. Choi, "Massive MIMO channel prediction: Kalman filtering vs. machine learning," *IEEE Trans. on Commun.*, vol. 69, no. 1, pp. 518–528, 2021.
- [24] Y. Lin, S. Jin, M. Matthaiou, and X. You, "Channel estimation and user localization for IRS-assisted MIMO-OFDM systems," *IEEE Trans. on Wireless Commun.*, vol. 21, no. 4, pp. 2320–2335, 2022.
- [25] Y. Lu and L. Dai, "Near-field channel estimation in mixed LoS/NLoS environments for extremely large-scale MIMO systems," *IEEE Trans. on Commun.*, vol. 71, no. 6, pp. 3694–3707, 2023.
- [26] L. V. Nguyen, D. H. N. Nguyen, and A. L. Swindlehurst, "Deep learning for estimation and pilot signal design in few-bit massive MIMO systems," *IEEE Trans. on Wireless Commun.*, vol. 22, no. 1, pp. 379–392, 2023.
- [27] H. Chung and S. Kim, "Location-aware beam training and multi-dimensional ANM-based channel estimation for RIS-aided mmwave systems," *IEEE Trans. on Wireless Commun.*, vol. 23, no. 1, pp. 652–666, 2024.
- [28] T. Li, X. Wang, P. Fan, and T. Riihonen, "Position-aided channel estimation for large-scale MIMO in high-speed railway scenarios," in *Proc. IEEE Global Commun. Conf. (GLOBECOM)*, pp. 1–6, Washington, DC, USA, 2016.
- [29] Y. Wang, Y. Wang, S. Zhang, and H. Cen, "Channel tracking and transmission design in 5G large-scale MIMO system," *IEEE Access*, vol. 7, pp. 62 032–62 041, 2019.
- [30] S. Taner, M. Guillaud, O. Tirkkonen, and C. Studer, "Channel charting for streaming CSI data," in *Proc. Asilomar Conf. Signals Syst Comput.*, pp. 1648–1653, 2023.
- [31] M. Stahlke, G. Yammine, T. Feigl, B. M. Eskofier, and C. Mutschler, "Velocity-based channel charting with spatial distribution map matching," *IEEE J. Indoor Seamless Position Navig.*, vol. 2, pp. 230–239, 2024.
- [32] S. Taner, V. Palhares, and C. Studer, "Channel charting in real-world coordinates," in *Proc. IEEE Global Commun. Conf.*, pp. 3940–3946, 2023.
- [33] Y. Zeng, J. Chen, J. Xu, D. Wu, X. Xu, S. Jin, X. Gao, D. Gesbert, S. Cui, and R. Zhang, "A tutorial on environment-aware communications via channel knowledge map for 6G," *IEEE Commun. Surveys Tuts.*, *arXiv preprint arXiv:2309.07460*, 2023, to appear.
- [34] D. Wu, Y. Zeng, S. Jin, and R. Zhang, "Environment-aware hybrid beamforming by leveraging channel knowledge map," *IEEE Trans. on Wireless Commun.*, pp. 1–1, 2023.
- [35] J. Wang, Q. Zhu, Z. Lin, J. Chen, G. Ding, Q. Wu, G. Gu, and Q. Gao, "Sparse bayesian learning-based hierarchical construction for 3D radio environment maps incorporating channel shadowing," *IEEE Trans. on Wireless Commun.*, pp. 1–1, 2024.
- [36] T. Choi, I. Kanno, M. Ito, W.-Y. Chen, and A. F. Molisch, "A realistic path loss model for cell-free massive MIMO in urban environments," in *Proc. IEEE Global Commun. Conf. (GLOBECOM)*, pp. 2468–2473, 2022.